Frequency-domain Triangulation for Single-Camera Sound Radiation Measurement

Domen Gorjup [1], *Sofia Baldini* [2], *Gianluca Guernieri* [2], *Paolo Gardonio* [2], *Janko Slavič* [1], *and Roberto Rinaldo* [2]

[1] University of Ljubljana, Faculty of Mechanical Engineering, domen.gorjup@fs.uni-lj.si

[2] Università degli Studi di Udine - DPIA

ABSTRACT

This paper presents the experimental findings of a novel, single-camera method for measuring sound radiation fields generated by structural vibrations, using high-speed imaging and the frequency-domain triangulation method. Traditional acoustic measurements, which are vital in fields ranging from machinery diagnostics to architectural acoustics, often require specialized facilities and complex experimental setups. In contrast, this study demonstrates a single camera based, non-contact approach that provides high spatial resolution and is suitable for in situ measurements. The method was tested on a baffled steel cylinder, excited in the frequency range up to 1500 Hz. By sequentially capturing high-speed video from 18 distinct viewpoints around the cylinder and applying frequency-domain triangulation on the DIC-computed displacements, we reconstructed its spatial operating deflection shapes at key frequencies. The camera-derived vibration data were used to model the sound radiation field, and validation tests with a laser vibrometer and microphone array showed close agreement between measurements. This method accurately captures the vibrational deflection shapes and essential features of the sound radiation field, avoiding spatial discretization limitations of traditional approaches while maintaining the potential of robust field applicability. This study offers a promising alternative to traditional vibro-acoustic measurement techniques with reduced experimental setup complexity, particularly in environments where physical access to the structure is an issue.

Keywords: Sound Radiation, ODS, Single-Camera, Multi-View, Frequency Domain Triangulation, DIC

1. INTRODUCTION

Sound radiation measurement is traditionally performed in controlled environments using specialized acoustic facilities. While these setups provide high accuracy, they are costly and impractical for in situ

applications. To overcome these limitations, alternative techniques have been developed, focusing on optical and image-based methods to reconstruct sound fields from structural vibrations.

Near-field acoustic holography [1] and beamforming [2, 3] with microphone arrays are commonly used approaches, with recent advancements improving spatial resolution and measurement efficiency. Machine learning has been used to further enhance acoustic imaging by refining source localization and noise suppression [4]. Optical methods provide a compelling alternative, offering high spatial resolution and non-contact measurement capabilities. Rohlfing et al. [5] demonstrated sound radiation estimation from laser vibrometry, while Gardonio et al. [6] proposed full-field optical vibration measurement using high-speed cameras, eliminating the need for scanning systems.

Image-based vibration measurement techniques, including digital image correlation (DIC) [7] and optical flow-based methods [8], have been widely used for structural analysis. 3D vibration fields are typically obtained using synchronized stereo-camera setups, though single-camera multi-view methods utilizing mirrors or frequency-domain triangulation offer a practical alternative [9, 10].

This study uses the frequency-domain triangulation method [11] to reconstruct sound radiation from the flexural vibrations of 3D shell structures. A fixed high-speed camera captures multi-view optical recordings as the structure is rotated, enabling full-field vibration estimation. The reconstructed vibrating response field is then used to compute sound radiation via a discretized Kirchhoff–Helmholtz integral [12]. An extended report on this research with a detailed discussion was recently published in a journal paper [13].

The paper is structured as follows: Section 2. describes the test setup, Section 3. introduces the theoretical background of the proposed method, and Section 4. presents the results with experimental validation against laser vibrometry and microphone array measurements.

2. MEASUREMENT SETUP

2.1. The observed structure

An experiment was conducted to validate the proposed method on a thin-walled steel cylinder with acoustic baffles. The specimen was a 1-mm-thick sheet-metal cylinder with a radius of 149 mm and a height of 296 mm, clamped at both ends by rigid flanges. Two cylindrical extensions were attached to act as acoustic baffles, as shown in Figure 1 (a), ensuring that the radiated sound could be derived analytically.

The structure was excited with a periodic pseudo-random broadband force signal, and its flexural vibrations were measured using the image-based method as well as using scanning laser Doppler vibrometry (LDV). These measurements were used further to reconstruct the structure's sound radiation fields using the proposed methodology. The vibration and acoustic fields were analysed at selected resonance frequencies. Due to the low modal overlap observed in the measured FRF, the operating deflection shapes (ODS) at peak vibration amplitudes closely resembled the resonant mode shapes. Similarly, the near-field acoustic radiation exhibited distinct lobes, mirroring the circular pattern of the flexural modes at each resonance frequency.

The cylinder was mounted on a base flange with a rotating joint, allowing it to be incrementally turned while keeping the measurement equipment — the optical high-speed camera and the laser Doppler vibrometer — stationary (Figure 1). All measurements were conducted across an audio frequency range of 20 to 1500 Hz. Due to the relatively lengthy scanning LDV measurement process, the experiments could not be performed simultaneously.

2.2. The imaging system

A Photron FASTCAM SA-Z high-speed camera (Figure 1 a) was used for image acquisition. A high-contrast speckle pattern was applied to the cylinder surface to facilitate Digital Image Correlation, with

two rows of ArUco markers printed along the top and bottom edges for automatic feature extraction and extrinsic calibration (Figure 1 b).

The cylinder was incrementally rotated around its vertical axis between consecutive recordings, capturing high-speed footage from 18 different viewpoints while subjected to stationary broadband random excitation. The same excitation signal was used in each measurement. A total of 50,000 12-bit monochrome images were recorded per viewpoint at 10,000 frames per second, with a resolution of 896 × 896 pixels, generating 1.31 terabytes of image data.
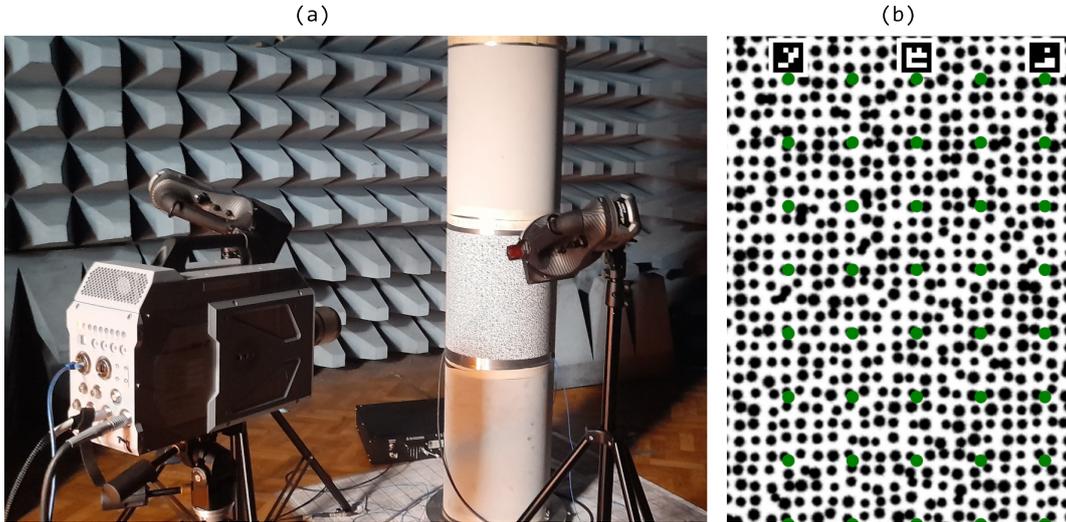

Figure 1: The camera measurement setup (a) and the high-contrast speckle pattern with ArUco markers and LDV targets (b).

The multi-view imaging system was calibrated in two stages. First, intrinsic camera parameters $\mathbf{K}$, including focal length and optical center, were determined from images of a standard checkerboard calibration pattern. Since the camera settings remained unchanged throughout the acquisition process, this step was only performed once.

Next, the ArUco markers in the recorded images were used alongside their known positions on the cylinder surface to perform extrinsic calibration. The Perspective-n-Point algorithm [14] was applied to compute the camera's rotation matrices $\mathbf{R}$ and translation vectors t for each of the 18 viewpoints, yielding a fully calibrated multi-view system with known projection matrices [15]:

$$\mathbf{P} = \mathbf{K}\,[\mathbf{R}|t] \tag{1}$$

The vibration and sound radiation fields reconstructed from the camera measurements were finally validated against measurements taken respectively with a scanning laser vibrometer and a microphone array.

3. SOUND RADIATION FROM MULTI-VIEW CAMERA MEASUREMENTS

3.1. Frequency-domain triangulation for single-camera spatial vibration measurement

The flexural vibrations of the cylinder were derived from monochrome digital images using the frequency-domain triangulation method introduced in [11]. This method reconstructs the full-field 3D operating deflection shapes (ODS) of a structure using a single camera. Unlike conventional vibration measurement techniques based on multi-camera photogrammetry [16], the approach implemented here relies on sequential recordings from a single camera while the structure is incrementally moved (rotated around the cylinder's vertical axis, in our case) between measurements, subjected to the same stationary excitation.

Careful selection of the broadband spectrum excitation profile ensures the structure's linear response, and the linearity in the frequency-domain of the observed small-displacement camera projections. The image-based displacements captured in each recording are transformed into the frequency domain, where triangulation is used to reconstruct the spatial displacement spectra. Each viewpoint is recorded in separate experiments, requiring only that the excitation remains stationary between measurements. The method is thus capable of reconstructing spatial ODS of linear, time-invariant systems under stationary excitation using a single moving camera. This is based on the equation (2) of perspective-camera projection (1) of small harmonic motion $\boldsymbol{U}(\omega)$ in the frequency domain [11]:

$$\boldsymbol{u}(\omega) = \frac{1}{w^{\mathrm{REF}}} \, \mathbf{P} \, \boldsymbol{U}(\omega), \tag{2}$$

illustrating that common triangulation techniques can be used to reconstruct spatial ODS from image-based displacement measurements $\boldsymbol{u}(\omega)$.

The frequency-domain triangulation 3D vibration measurement method can be summarized by the four steps, illustrated in Figure 2.
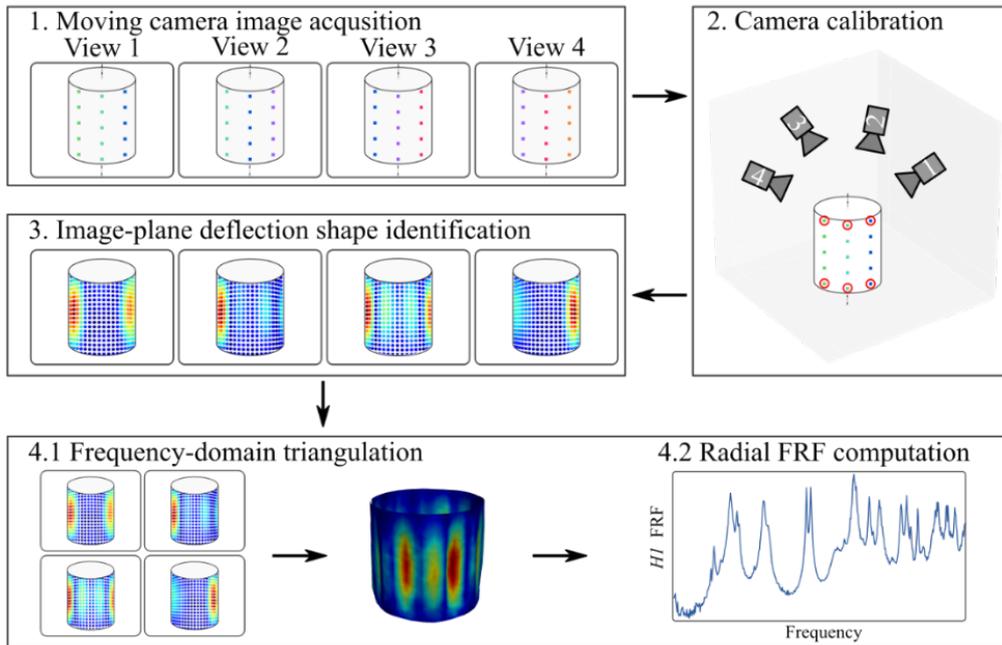

Figure 2: The single-camera multi-view frequency-domain triangulation procedure of measuring spatial vibrations.

From the reconstructed spatial ODS at each observed point in space, $\boldsymbol{U} = (u, v, z)^T$, the complex amplitude of the radial displacement u_r in the direction, normal to the cylinder surface, $\boldsymbol{n}$, can be extracted using the simple projection:

$$u_r(\omega) = \frac{\boldsymbol{U}(\omega) \cdot \boldsymbol{n}}{|\boldsymbol{n}|}, \tag{3}$$

and the radial velocity w_r can simply be constructed by using frequency-domain derivation of the result:

$$w_r(\omega) = \mathrm{j}\,\omega\,u_r(\omega). \tag{4}$$

3.2. Sound radiation field reconstruction

The sound radiation field was reconstructed using the Kirchhoff-Helmholtz integral formulation for the sound pressure $p(x_i, \omega)$ at position $x_i = (r_i, \theta_i, z_i)$, from the camera-measured velocities measured at

the selected grid points $x_c = (r_c, \theta_c, z_c)$ (expressed in cylindrical coordinates):

$$p(x_i, \omega) = -\int_{S_c} \left(p(x_c, \omega) \frac{\partial g(|x_i - x_c|, \omega)}{\partial r} + j\,\omega\,\rho_0\,g(|x_i - x_c|, \omega)\,w_r(x_c, \omega) \right) dS_c, \qquad (5)$$

where ρ_0 is the surrounding air density, S_c the surfaces of the cylinder and the baffles and $g(|x_i - x_c|, \omega)$ the free-space 1st - kind Green function.

For the baffled cylinder structure, considered in this study, and using a Riemann sum approximation of radiating pistons at the point grid centres, the integral formulation can be further simplified. Due to the lengthy derivation, the reader is kindly directed to the original publication [13] for the final result.

4. RESULTS

Figure 3 compares the total flexural kinetic energy spectra in the observed frequency range, measured by the scanning laser vibrometer and the camera-based method. Comparing the two spectra, a good agreement between the two methods can be observed, especially in the lower frequency range. The small frequency shift of some of the observed resonant peaks is possibly due to the varying environmental conditions (namely a several degree temperature change) between the two measurements. A representation of the camera-based spatial deflection shapes at the identified resonant peaks can also be seen in Figure 3.
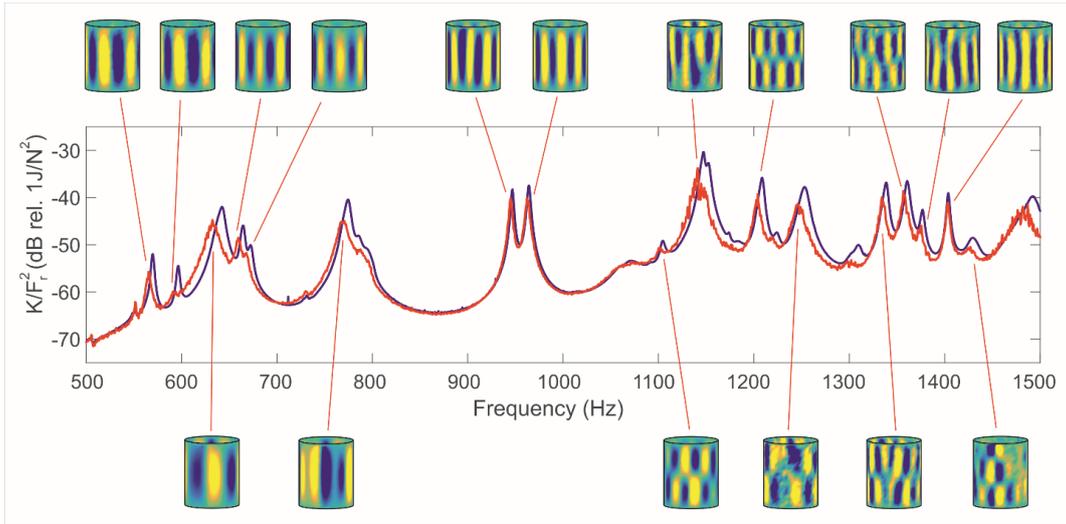

Figure 3: The laser (violet) and camera (red) measured total flexural kinetic energy spectra with camera-based ODS at resonant peaks.

Using the Kirchhoff-Helmholtz formulation (KH), described in Section 3.2. and [13], the LDV and camera-based velocities were also used to reconstruct the sound radiation fields. Figure 4 shows a comparison between the camera (a), laser (b) and microphone array (c) sound radiation reconstructions. It is evident that the agreement, especially, between the camera and LDV measurements, is excellent, and the two optical methods produce results comparable to the acoustic (microphone array) measurement.

5. CONCLUSIONS

This study presents the possibility of using the frequency-domain triangulation spatial vibration measurement method to measure surface velocity of thin-walled structures and reconstruct the sound radiation field using the Kirchhoff-Helmholtz formulation. The single-camera image-based measurement approach exhibits clear advantages over acoustic measurements, the principal contribution being the high
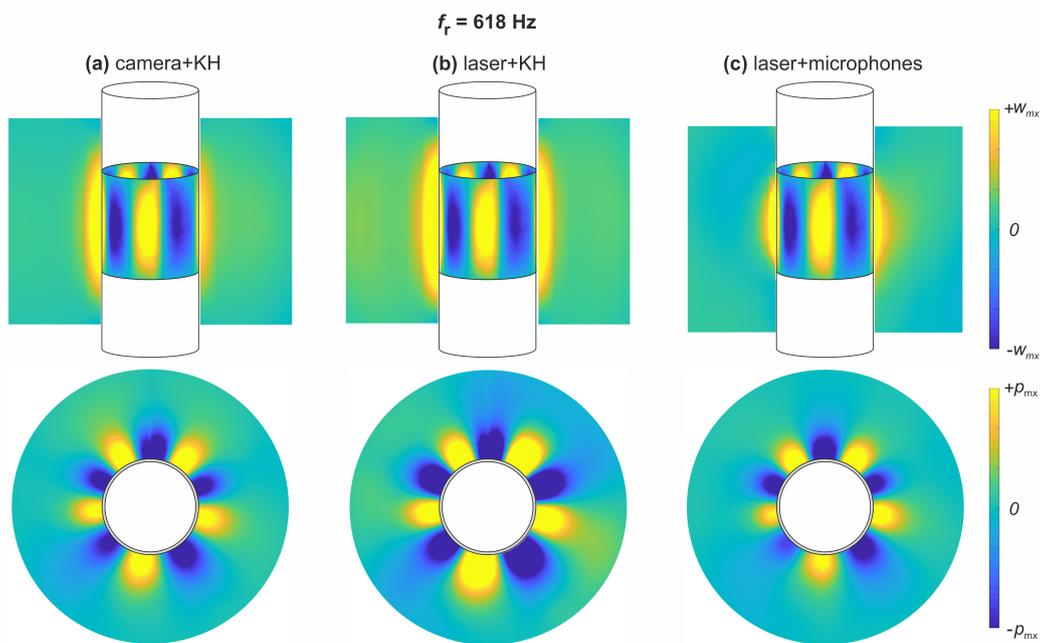
Figure 4: The camera (a), laser (b) and laser + microphones measured vibration and sound radiation fields at 618 Hz.

spatial resolution of the result as well as the possibility of longer-range data acquisition with less strict environmental condition requirements, enabling in situ sound radiation measurements. It also offers multiple advantages over established vibration measurement methods (e. g. accelerometers or LDV), such as lower complexity of the measurement setup and much faster data acquisition, in addition to offering full-field results. This comes at the expense of relatively long processing times and lower measurement dynamic range. Nevertheless, the presented results show that the camera-based approach can offer a good alternative to these conventional experimental methods.

ACKNOWLEDGMENTS

REFERENCES

[1] M.B. Salin and D.A. Kosteev. Nearfield acoustic holography-based methods for far field prediction. *Applied Acoustics*, 159:107099, February 2020. ISSN 0003-682X. doi: 10.1016/j.apacoust.2019. 107099. URL http://dx.doi.org/10.1016/j.apacoust.2019.107099.

[2] U. Michel. History of acoustic beamforming. In *1st. Berlin Beamforming Conference*, 2006. URL https://elib.dlr.de/47021/.

[3] Fangli Ning, Di Meng, and Juan Wei. An improved acoustic imaging algorithm combining object detection and beamforming for acoustic camera. *JASA Express Letters*, 2(6), June 2022. ISSN 2691-1191. doi: 10.1121/10.0011735. URL http://dx.doi.org/10.1121/10. 0011735.

[4] Pengwei Xu, Elias J.G. Arcondoulis, and Yu Liu. Acoustic source imaging using densely connected convolutional networks. *Mechanical Systems and Signal Processing*, 151:107370, April 2021.

ISSN 0888-3270. doi: 10.1016/j.ymssp.2020.107370. URL http://dx.doi.org/10.1016/j.ymssp.2020.107370.

[5] J. Rohlfing, P. Gardonio, and D.J. Thompson. Comparison of decentralized velocity feedback control for thin homogeneous and stiff sandwich panels using electrodynamic proof-mass actuators. *Journal of Sound and Vibration*, 330(5):843–867, February 2011. ISSN 0022-460X. doi: 10.1016/j.jsv.2010.09.013. URL http://dx.doi.org/10.1016/j.jsv.2010.09.013.

[6] Paolo Gardonio, Roberto Rinaldo, Loris Dal Bo, Roberto Del Sal, Emanuele Turco, and Andrea Fusiello. Free-field sound radiation measurement with multiple synchronous cameras. *Measurement*, 188:110605, January 2022. ISSN 0263-2241. doi: 10.1016/j.measurement.2021.110605. URL http://dx.doi.org/10.1016/j.measurement.2021.110605.

[7] T. C. Chu, W. F. Ranson, and M. A. Sutton. Applications of digital-image-correlation techniques to experimental mechanics. *Experimental Mechanics*, 25(3):232–244, Sep 1985. ISSN 1741-2765. doi: 10.1007/BF02325092. URL https://doi.org/10.1007/BF02325092.

[8] Jaka Javh, Janko Slavič, and Miha Boltežar. The subpixel resolution of optical-flow-based modal analysis. *Mechanical Systems and Signal Processing*, 88:89 – 99, 2017. ISSN 0888-3270. doi: https://doi.org/10.1016/j.ymssp.2016.11.009. URL http://www.sciencedirect.com/science/article/pii/S0888327016304770.

[9] Liping Yu and Bing Pan. Single-camera high-speed stereo-digital image correlation for full-field vibration measurement. *Mechanical Systems and Signal Processing*, 94:374 – 383, 2017. ISSN 0888-3270. doi: https://doi.org/10.1016/j.ymssp.2017.03.008. URL http://www.sciencedirect.com/science/article/pii/S088832701730122X.

[10] Domen Gorjup, Janko Slavič, Aleš Babnik, and Miha Boltežar. Still-camera multiview spectral optical flow imaging for 3d operating-deflection-shape identification. *Mechanical Systems and Signal Processing*, 152:107456, May 2021. ISSN 0888-3270. doi: 10.1016/j.ymssp.2020.107456. URL http://dx.doi.org/10.1016/j.ymssp.2020.107456.

[11] Domen Gorjup, Janko Slavič, and Miha Boltežar. Frequency domain triangulation for full-field 3d operating-deflection-shape identification. *Mechanical Systems and Signal Processing*, 133:106287, 2019. ISSN 0888-3270. doi: https://doi.org/10.1016/j.ymssp.2019.106287. URL http://www.sciencedirect.com/science/article/pii/S0888327019305023.

[12] Frank Fahy and Paolo Gardonio. *Sound and Structural Vibration*. Academic Press, San Diego, CA, 2 edition, November 2006.

[13] Sofia Baldini, Gianluca Guernieri, Domen Gorjup, Paolo Gardonio, Janko Slavič, and Roberto Rinaldo. 3d sound radiation reconstruction from camera measurements. *Mechanical Systems and Signal Processing*, 227:112400, March 2025. ISSN 0888-3270. doi: 10.1016/j.ymssp.2025.112400. URL http://dx.doi.org/10.1016/j.ymssp.2025.112400.

[14] Francesc Moreno-Noguer, Vincent Lepetit, and Pascal Fua. Accurate non-iterative o(n) solution to the PnP problem. *2007 Ieee 11Th International Conference On Computer Vision, Vols 1-6*, pages 2252–2259, 2007. URL http://infoscience.epfl.ch/record/179767.

[15] Richard Hartley and Andrew Zisserman. *Multiple View Geometry in Computer Vision*. Cambridge University Press, New York, NY, USA, 2 edition, 2003. ISBN 0521540518.

[16] Javad Baqersad, Peyman Poozesh, Christopher Niezrecki, and Peter Avitabile. Photogrammetry and optical methods in structural dynamics – a review. *Mechanical Systems and Signal Processing*, 86: 17 – 34, 2017. ISSN 0888-3270. doi: https://doi.org/10.1016/j.ymssp.2016.02.011. URL http://www.sciencedirect.com/science/article/pii/S0888327016000388. Full-field, non-contact vibration measurement methods: comparisons and applications.